WIND ENERGY
Wind Energ. 2013; **00**:1–14
DOI: 10.1002/we

RESEARCH ARTICLE

Validation of boundary layer parameterization schemes in the Weather Research and Forecasting model (WRF) under the aspect of offshore wind energy applications - Part II: Boundary layer height and atmospheric stability

O. Krogsæter[1] and J. Reuder[2]

[1] StormGeo AS, Nøstekaien 1, 5011 Bergen, Norway.
[2] Geophysical Institute, University of Bergen, Allégaten 70, 5020 Bergen, Norway.

ABSTRACT

Five different Planetary Boundary Layer (PBL) schemes in the Weather Research and Forecasting model (WRF) have been tested with respect to their capability to model boundary layer parameters relevant for offshore wind deployments. For the year 2005 model simulations based on the YSU, ACM2, QNSE, MYJ, and MYNN2 PBL schemes with WRF have been performed for the North Sea and validated against measurements of the FINO1 platform. In Part I the investigations had focus on the key parameters 100 m mean wind speed and wind shear in terms of the power-law exponent. In part II the focus is now set on the capability of the model to represent height and stability of the marine atmospheric boundary layer. Considerable differences are found among the PBL-schemes in predicting the PBL-height. A substantial part of this variation is explained by the use of different PBL-height definitions in the schemes. The use of a standardized procedure in calculating the PBL height from common WRF output parameters, in particular the temperature gradient and the wind shear, leads to reduced differences between the different schemes and a closer correspondence with the FINO1 measurements. The study also reveals a very clear seasonal dependency of the atmospheric stability over Southern North Sea. During winter time the marine atmospheric boundary layer is more or less neutral with several episodes of unstable periods. During spring and early summer the occurrence of periods with very stable stratification becomes dominant with stable conditions up to 40-45% of the time when warm continental air is advected from the South. In general the results of part II confirm again that the MYJ scheme performs slightly better than the others and can therefore be suggested as first choice for marine atmospheric boundary layer simulations without a-priori information of atmospheric stability in the region of interest.

KEYWORDS

Marine atmospheric boundary layer; parameterization; WRF; FINO1; PBL-height; stability.

Correspondence
StormGeo AS, Nøstekaien 1, 5011 Bergen, Norway.
E-mail: olav.krogsaeter@stormgeo.com

Received . . .

Prepared using weauth.cls [Version: 2010/06/17 v1.00]

1. INTRODUCTION

In part I the investigations were focused on how different Planetary Boundary Layer (PBL) schemes in The Weather Research and Forecasting (WRF) model simulate wind speed and wind profiles in offshore conditions in the Southern North Sea in comparison to the measurements at the FINO1 platform. For the average wind speed at 100 m, the approximate hub height of modern offshore wind turbines, only subtle differences in the yearly statistics among the schemes were found. A more detailed investigation revealed larger deviations for wind speeds above 15 ms^{-1}, where most of the schemes clearly overestimated the frequency of occurrence of strong winds. In this context the MYJ scheme showed the best performances over the whole wind speed range and the different atmospheric stability classes. Larger deviations were found in the wind shear, expressed in terms of the Hellmann exponent in the power-law. The ability of the different schemes in predicting the wind shear reveals a strong dependency on atmospheric stability. But again, the MYJ scheme performed overall best, producing reasonable results for most of the situations (except for very stable conditions), while the other schemes are characterized by a distinctly higher variability in their skills from one stability class to another.
The understanding and interpretation of these observations and results requires a more thorough investigation of the complex structure of the Marine Atmospheric Boundary Layer (MABL) in particular with respect to the relevant turbulent exchange processes of heat and momentum that determine the interaction between atmospheric stability and wind shear. The PBL height is one of the key parameters while modeling the boundary layer, as the PBL-schemes need this information in order to calculate the mixing of heat, humidity, and momentum in an adequate way. This again determines the vertical profiles of temperature, humidity and wind.
While there are quite a number of research papers dealing with PBL-height over land, [1],[2], [3],[4]. or coastal regions [5], [6],[7],[8], only few studies are available on the offshore marine PBL-height. This is not surprising as good offshore observations are infrastructurally demanding and difficult to obtain. In addition that topic had not been in the main research focus until larger scale offshore wind installations have been planned and developed. The first detailed study on the growth of the stable boundary layer over sea (warm air over a cool sea) was not published before 1987, [9]. The growth rate is reported to be very slow, and it requires a fetch of several hundreds of kilometers to develop a PBL-height of several hundreds of meters. One of the newest marine studies, [6], is done at a coastal site in Denmark, determining the PBL-height in offshore wind conditions, by the use of a wind lidar, an aerosol lidar, a ceilometer, a met mast, and model outputs from WRF. However the study is covering only a few days with westerly offshore wind conditions during a two month period. One of the main findings is that the direct computations of the PBL-height from WRF using the YSU scheme tend to underestimate the PBL-height.
PBL-height and atmospheric stability are closely related to each other and play both a crucial role in the characterization of the Marine Atmospheric Boundary Layer (MABL). A study from Vindeby in Denmark [10] shows that the impact of stability on the wind profile is more pronounced at low wind speeds, where the frequency of the different stratification classes in the boundary layer is evenly divided into unstable and stable classes. For above 12 ms^{-1} the observations mostly show a near-neutral boundary layer profile. The fetch from land has also a strong influence on the frequency of the different stability classes, with a significant higher occurence of stable stratification with wind from land, and more neutral and unstable stratification classes with wind from ocean. In another study, [11], an expression for the wind speed profile was compared with LIDAR measurements (161 m.a.s.l) and met mast measurements (45 m.a.s.l.), from an offshore site 18 km west of Denmark. It showed good results, except for the stable MABL, but by adding the PBL-height to the expression the results were significantly improved. It is also found that the wind shear is significantly higher from measurements at e.g. Horns Rev and FINO1 compared with mesoscale model simulations, [12], and that one important reason is the effect of atmospheric stability.

The simulations in this study are done with The Weather Research and Forecasting model (WRF) version 3.2.1. The domain setup consists of three two-way nested domains with 27, 9 and 3 km grid spacing with the innermost domain covering the southern part of the North Sea. The main task is to test the performance of the various parameterization schemes on the marine boundary layer. Five different PBL-schemes in WRF, the YSU, ACM2, QNSE, MYJ, and MYNN2

Wind Energ. 2013; **00**:1–14 © 2013 John Wiley & Sons, Ltd.
DOI: 10.1002/we
Prepared using weauth.cls

scheme, have been used in this study. Each PBL-scheme is run for the full year of 2005 with otherwise constant setup and boundary conditions. The model simulations are verified against the observational dataset available from the research platform FINO1 [13]. FINO1 is located at 54.01N, 6.59E, about 45 km north of the German coast in the Southern North Sea. The year 2005 was chosen because of the most complete dataset available at the time the study was initiated. As no temperature data were available for a longer period in August, this month lacks reliable information on measured surface layer stability and has been excluded from the investigations. More details on model setup and observational data can be found in: "Part I: Average wind speed and wind shear."

2. STABILITY CLASSIFICATION

A consistent treatment of the stability calculation both for measurements and model results is required. In the following the Pasquill-Gifford-Turner (PGT) stability classification method has been used. It was originally developed in the beginning of the 1960s to compute the dispersion coefficients used in air quality models for the prediction of the concentration of pollutants [19], [20]. The classification was originally based on SYNOP observations of wind speed and solar insolation/cloudiness, and divided the atmospheric stability into seven classes from 'A - Very unstable' to 'G - Very stable'. During the following decades more quantitative schemes have been developed and applied to assess the PGT stability classification (e.g. [21]). It turned out that the algorithms based on the Monin-Obukhov length L and the gradient Richardson number Ri_g showed the best performance. This is not surprising as those methods include both thermally and mechanically induced turbulence, and not just one of the mechanisms.

As all required parameters for the advanced methods are available from both the measurements at FINO1 and the model simulations, the Ri_g method has been choosen for the following investigation. Ri_g has been calculated as (see also eq. 8):

$$Ri_g = \frac{g(\Delta\Theta_v/\Delta z)}{\overline{\Theta_v}(\Delta U/\Delta z)^2} \tag{1}$$

where g is the gravitational constant, $\Delta\Theta_v$ is the virtual potential temperature difference between 40 m and 100 m. $\Delta z = 60m$, $\overline{\Theta_v}$ the average virtual potential temperature between 40 m and 100 m, and ΔU the wind speed difference between 40 m and 100 m.

The limits of Ri_g for the different stability classifications come from:

$$Ri_g = \frac{z/L\phi_h}{\phi_m^2} \tag{2}$$

where ϕ_h is the non-dimensional temperature profile and ϕ_m is the non-dimensional wind profile. For 'A - Very unstable' to 'E - Weakly stable' conditions the Businger formulation for ϕ_h and ϕ_m is used:

For $z/L < 0$ (unstable/neutral):

$$\phi_m = 0.74(1 - 9z/L)^{1/2} \tag{3}$$

$$\phi_h = (1 - 15z/L)^{1/4} \tag{4}$$

for $0 < z/L < 0.5$ (neutral/weakly stable):

$$\phi_m = 0.74 + 4.7z/L \tag{5}$$

$$\phi_h = 1 + 4.7z/L \tag{6}$$

Table I. PGT stability classes

Stability classes	Ri_g limits
A, very unstable	$Ri_g < -5.34$
B, unstable	$-5.34 <= Ri_g < -2.26$
C, weakly unstable	$-2.26 <= Ri_g - 0.569$
D, neutral	$-0.569 <= Ri_g < 0.083$
E, weakly stable	$0.083 <= Ri_g < 0.196$
F, stable	$0.196 <= Ri_g < 0.49$
G, very stable	$Ri_g >= 0.49$

For 'F - Stable' and 'G - Very stable' the Hick formulation is used.
For $z/L >= 0.5$ (stable)

$$\phi_m = \phi_h = 8 - \frac{4.25}{z/L} + \frac{1}{(z/L)^2} \tag{7}$$

The Hick formulation has been chosen for the stable cases based on earlier studies indicating better results in stably stratified layers compared with the Businger formulation, [22]. The limits in terms of the Ri_g number, are then estimated from the nomogram of Golder, [23], which relates L to the PGT stability classes presented in table I.

One of the most important parameter in PBL-modeling is its height. It determines the upper boundary of the PBL, and hence the vertical extension of turbulent mixing of momentum, heat, and moisture. It consequently interacts with atmospheric stability and the shape of the wind profile expressed by the wind shear. Correct PBL height determination is important since it will affect the coherency of the turbulent structures over the rotor disk. A wide range of different definitions of the PBL-height exist in boundary layer meteorology, with some of the most common ones listed below:

- the height of a capping inversion.
- the height where the turbulence intensity falls below a certain threshold.
- the height of minimum heat flux.
- the height of maximum momentum (for Stable Boundary Layers, SBL, with associated low level jets).
- the height where the wind becomes geostrophic.
- the height where TKE goes below a specified threshold.
- the height where the local Richardson number exceed a critical Richardson number, R_c.

In the tested PBL-schemes the two last definitions are used for the PBL depth determination. The YSU scheme uses $R_c = 0.0$, while ACM2 and MYNN2 apply $R_c = 0.25$. The choice of R_c has been highly debated, and some papers argue strongly towards R_c in the order of one for the stably stratified atmosphere [14], [15]. The MYJ and QNSE schemes utilize a TKE threshold as definition. The top of the PBL in these schemes is reached when the TKE falls below a value of 0.2 $m^2 s^{-2}$ for the MYJ and 0.01 $m^2 s^{-2}$ for QNSE. Note the large difference in the thresholds by a factor of 20.

In the following results from modeled and observed boundary layer height, and stability classification computations are presented.

3. RESULTS

3.1. Modeled PBL-height.

Figure 1 presents the probability density distribution of the PBL height for each month of the year 2005 based on 1 hour values calculated by the different PBL schemes, using their implicit PBL-height definition. The results show a distinct seasonal variation in the PBL-height modeled with WRF for the position of FINO1. Spring, summer and the first autumn months are characterized by a bi-modal distribution, with a prominent peak for PBL heights of around 200-300 m, indicating stable conditions when relatively warm air is advected over the colder water. For March, May and

Wind Energ. 2013; **00**:1–14 © 2013 John Wiley & Sons, Ltd.
DOI: 10.1002/we
Prepared using weauth.cls

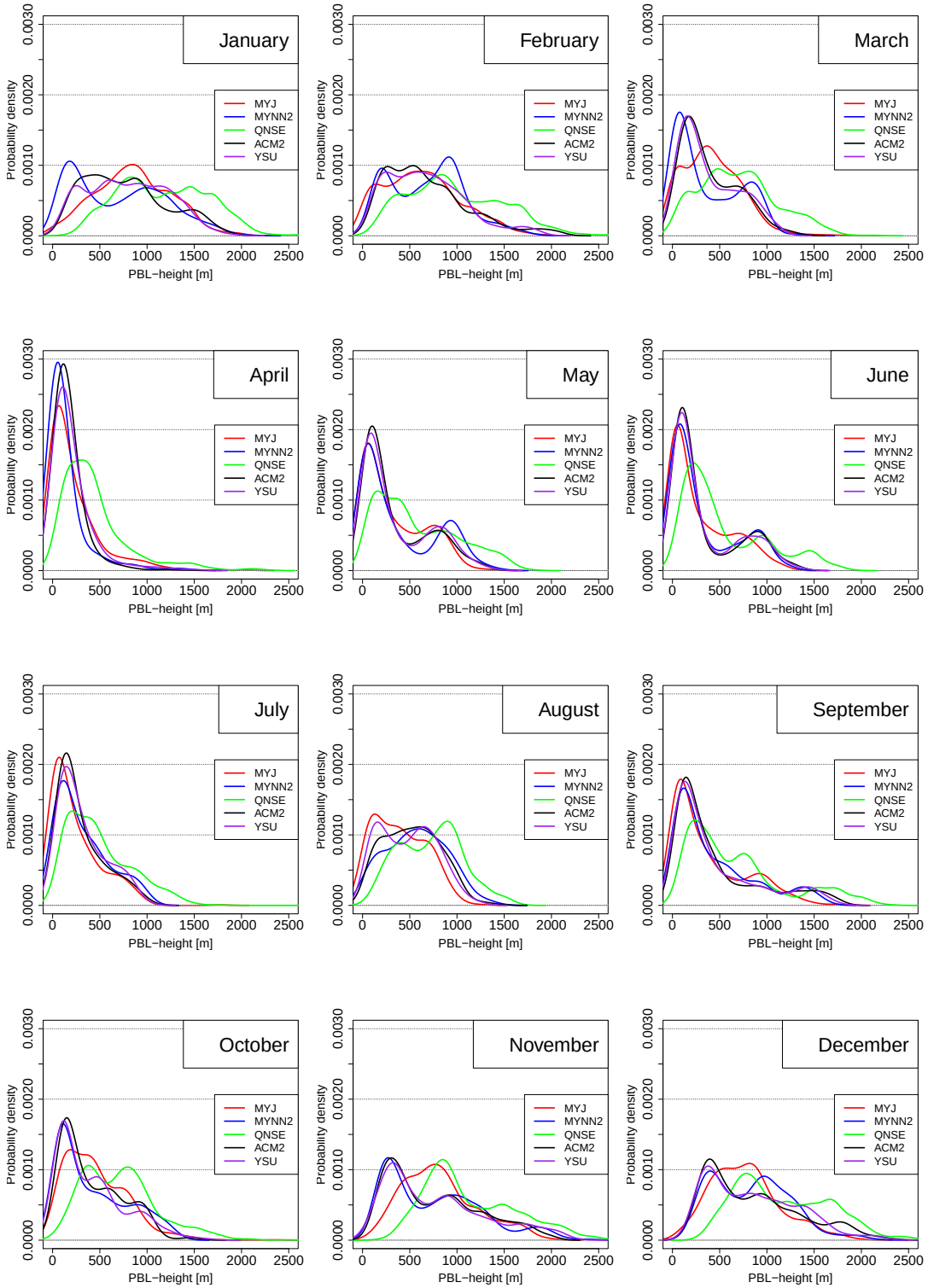

Figure 1. Monthly probability density distributions of modeled PBL-height at FINO1 for the year 2005.

June, a secondary clear peak can be found for PBL depths of 800-1000 m. The origin of this feature could be related to the existence of Stratocumulus-topped boundary layers, typically extending to these levels, [16], or to cloud free or cumulus topped boundary layers. During late autumn and winter the probability distribution is much broader, shifted towards higher PBL depths and is lacking the clear peaks of the summer months. This is indicating the higher probability of neutral to unstable conditions, caused by in average stronger winds during these seasons, and by the switch in sign in the difference between average air and sea temperatures. The year 2005 shows a sharp transition between February and March and a slower gradual transition in fall from September to November. If this is a climatological feature or a specific characteristic of this year can not be deduced from a one year data set. August represents a clear exception from the general behavior described above. The distribution here is rather uniform between ca. 200-1000 m. Reason for this was an exceptionally high low-pressure activity with average wind speeds far above the climatological mean for this month.

Despite the different definitions of the PBL height, four of the tested schemes (MYJ, MYNN2, ACM2, YSU) behave rather similar, with a slight tendency for the MYJ scheme to predict the lowest boundary layer in stable conditions during spring and summer. The QNSE scheme on the other hand differs systematically. Its probability density distribution is distinctly shifted towards higher PBL values. The peak for stable conditions in the warm season is lower, broader and also shifted by several hundreds of meters. This behavior becomes even more prominent when looking at fig. 2 that shows monthly values for the mean and first and third quartile of the distributions presented in fig. 1. Here it is obvious that QNSE on average predicts PBL heights that are 300-500 m higher than those of the other schemes. This is a direct effect of the choice of the low TKE threshold value of 0.01 $m^2 s^{-2}$ for calculating the PBL depth, while the TKE threshold value for MYJ is twenty times higher, 0.20 $m^2 s^{-2}$, and thus give very similar PBL heights as the other PBL-schemes. Similar behavior of QNSE has previously been reported in other studies, [17]. The monthly plot again reveals the very specific conditions for August, leading to PBL heights of several hundred meters higher than for the neighboring months.

Over the ocean the surface energy balance, and consequently the PBL height, is mainly determined by the difference between air and water temperature and shows typically no or only a weak diurnal cycle. Therefore it should be possible to use the PBL-height as a proxy for a division into stable and unstable atmospheric stratification. Over land this is most likely not applicable because the PBL height is coupled to fast changes in the diurnal surface energy balance, therefore a low PBL-height over land can be associated with both stable conditions but also with a rapidly growing convective boundary layer after sunrise.

A look at fig. 2 a) suggests that the mean of the PBL height can act as an indicator for the prevailing stability conditions of the corresponding month. A value of 200-400 m characterizes the clearly stable PBL from April to July. Monthly mean of PBL depths of more than 700 m (January, February, November, December) mean mainly neutral or unstable conditions. The third class in between corresponds to the transitional conditions and covers in 2005 the months of March, and August to October.

3.2. Observed PBL-height

A test and verification of the modeled PBL heights, presented in the section above, against the FINO1 data is limited to PBL heights lower than 100 m, i.e. stable conditions. It also requires a standardized procedure for the stability calculations that is applicable both to the model results and to the FINO1 measurements. The surface bulk Richardson number Ri_{bs}, defined as:

$$Ri_{bs} = z\frac{g}{\overline{\Theta}_v}\frac{\Delta\Theta_v}{U(z)^2} \tag{8}$$

has been chosen for this purpose. z denotes the height above surface (100 m), g the gravitational constant, and $\overline{\Theta}_v$ the average virtual potential temperature between the surface and z. $\Delta\Theta_v$ is the virtual potential temperature difference between z and the surface, and $U(z)$ the wind speed at level z. To compute Θ_v, pressure and humidity are also needed, which are all available from both WRF and FINO1.

DOI: 10.1002/we
Prepared using weauth.cls

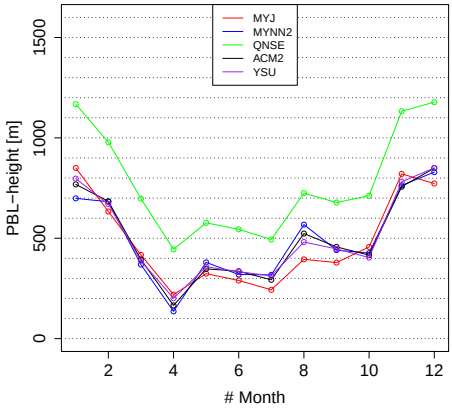

(a) Mean

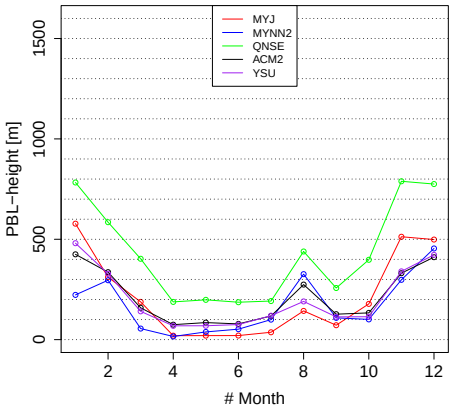

(b) First quartile

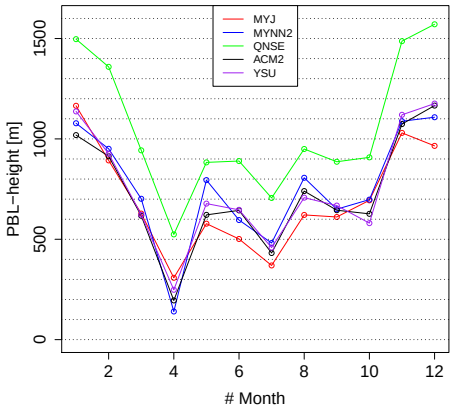

(c) Third quartile

Figure 2. Monthly modeled PBL-height at FINO1 for the year 2005.

At FINO1 the sea surface temperature (SST) is not directly measured, and the atmospheric temperature measurements start at an altitude of 30 m. To determine Θ_v at the surface, the temperature from measurements at 3 m below sea surface at FINO1 has been used instead of SST. It is known that both cool-skin and warm-layer effects may influence the SST, which will not be captured in measurements from deeper in the ocean [18]. In 2010 simultaneous measurements of temperature 3 m below sea level temperature and SST are available for one and a half month during summer. Those time series show up to 3 K temperature differences for very short time periods in connection with calm and sunny weather, when the ocean mixed layer is warming due to absorption of solar radiation. During cloudy or windy weather, the observed temperature difference is very small. As such conditions prevail most of the time, the use of the temperature 3 m below sea level instead of SST should not change the main interpretation of the results.

For the following investigations a critical value of $Ri_c = 0.3$ has been applied. This is the most commonly used value for such computations, and fits also into the values in table III. However, a few studies show that there is evidence for R_c is in the order of one for the stably stratified atmosphere, [14], [15]. Ri_{bs} has been calculated once per hour for the measurements and model calculations of the different PBL schemes. Consequently the PBL height h is below the mast top at $z = 100$ m each time when Ri_{bs} exceeds Ri_c.

Table II. $N1$ = number of time steps with PBL-heigh below 100 m computed from Richardson bulk number method with $R_c = 0.3$. $N2$ = number of time steps with PBL-height below 100 m computed with the implicit PBL-height definition of the schemes.

	April		May		June		July	
	$N1$	$N2$	$N1$	$N2$	$N1$	$N2$	$N1$	$N2$
FINO1	95		122		124		110	
YSU	42	215	82	249	27	191	8	124
ACM2	45	219	77	225	23	194	12	111
QNSE	32	36	74	77	24	17	9	17
MYNN2	48	354	78	260	38	199	10	156
MYJ	37	276	77	243	20	249	20	274

The results of the PBL-height calculations for the most stable months (April to July) are presented in fig. 3 and table II. Fig. 3 displays the occurrence of time steps with PBL-height below 100 m for every PBL-scheme tested, together with the FINO1 data. The figure shows huge differences among the models depending on the method of PBL-height determination in the different schemes. However, the first impression from the figure is that the PBL-schemes and the observations have PBL-height below 100 meter at least generally in the same periods. However, the PBL-height taken directly from the WRF output (red points) has in general a distinctly higher fraction of stable cases with PBL-height below 100 m than observed at FINO1. A clear exception is QNSE, which not only has fewer time steps than the other schemes, but even significantly fewer than the FINO1 data. The situation changes completely when the Richardson bulk number method is used also on the data of the schemes (black points), to be consistent with the method used for the FINO1 observations. Now the different schemes are rather similar to each other, but show a clear underestimation compared with the FINO1 data. These results are also quantified in table II. For the PBL-height computed by the implicit method of the schemes, the MYNN2 scheme, and partly the MYJ scheme, have a factor of 2-4 higher occurrence of time steps with PBL-height below 100 m than the FINO1 data, indicating a clear over-representation of the stable situations. YSU and ACM2 overestimate by a factor of 1.5 to 2, except for July where these two schemes match the observations nearly perfect. The exception is the QNSE-scheme, which only shows 15 to 60 $\%$ of PBL-height cases below 100 m compared to the observations from FINO1. This is also in agreement with the results presented in fig. 2. Using the bulk Richardson number method on all of the schemes, the occurrence of PBL-height below 100 meter ranges from only 10 $\%$ (July) to 60 $\%$ (May) compared with the FINO1 data. Since Ri_{bs} is not a direct result from measurements it is maybe not a reliable indicator by itself. The better correlation obtained when using the same indicator implies that the temperature gradient in the simulations is well predicted, but this is not tested explicitly.

When comparing modeled PBL-height with measurements these results show that it is of high importance to be aware of which methods are used for the computations. Using inconsistent methods can result in significant errors. It also shows, as in paper I, that the PBL-schemes have generally large difficulties regarding very stable atmospherical boundary layers.

3.3. Modeled and observed PGT stability classification.

The annual course of the PBL-height indicates the importance of atmospheric stability, raising interest in a more thorough investigation on this topic. Atmospheric stability, turbulence structure and intensity, and wind shear in the PBL are closely related to each other. For wind energy applications it is important to keep in mind that large turbulence intensity and large wind shear have both negative effects on wind turbines, as they reduce the power production at a given wind speed and increase fatigue loads leading to shorter lifetime of the installations. It is therefore interesting to see how well the different PBL schemes are able to model various stability conditions.

Fig. 2 showed a clear annual course in the average PBL-height calculated by the WRF model, with low values during spring and early summer and a distinct increase towards autumn and winter. The stability analysis of the FINO1 data and the model simulations presented in fig. 4 is in agreement with this finding. It shows that the frequency of occurrence of very stable atmospheric conditions is high during spring and early summer, while those situations are very rare during autumn and winter. This agreement explains that the PBL-height can act as a reasonable proxy for atmospheric stability in

DOI: 10.1002/we
Prepared using weauth.cls

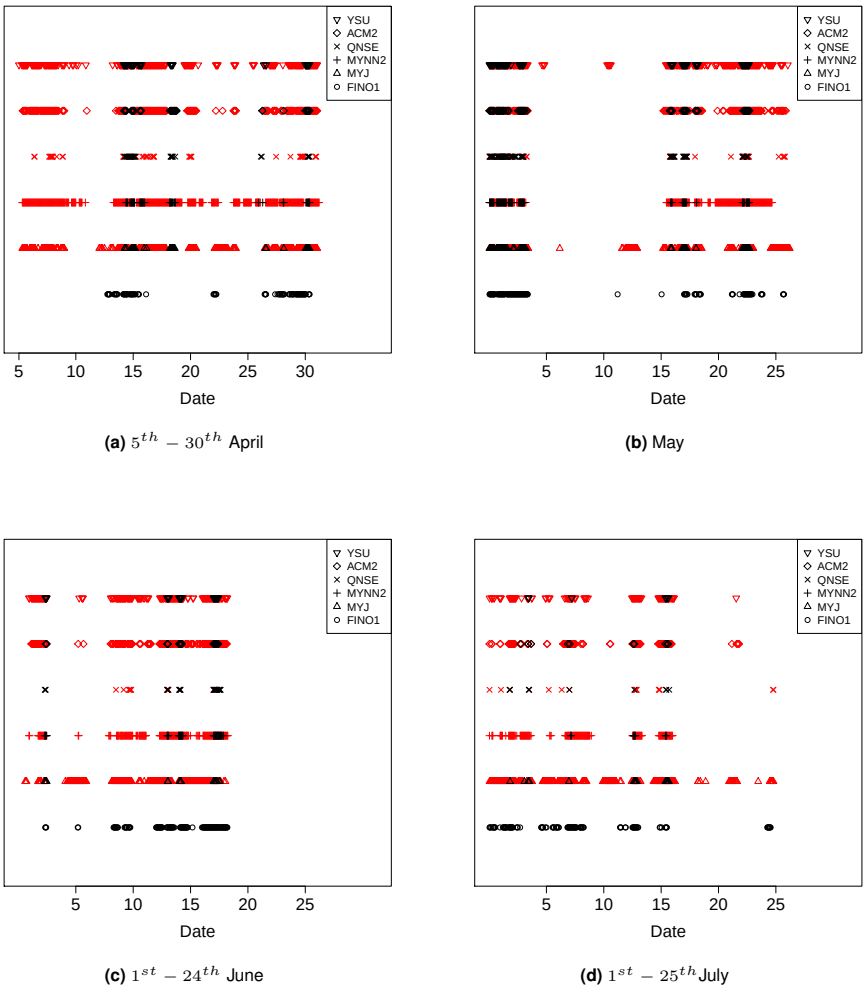

(a) $5^{th} - 30^{th}$ April **(b)** May

(c) $1^{st} - 24^{th}$ June **(d)** $1^{st} - 25^{th}$July

Figure 3. Hourly timesteps with PBL-height below 100 m at FINO1. Black color indicates the results from estimating the PBL-height with the bulk Richardson number method, with $Ri_c = 0.3$, on both FINO1 and the PBL-schemes. Red color represent the results taken directly from the WRF simulations using the implicit PBL-height definition. The different rows are for the different schemes, in the same order as written in the label inlays, while the FINO1 results are presented in the bottom row.

the MABL. PBL-height calculations vs. stability classes show that for the unstable classes, A-C, the mean PBL-height is 650 m, for the neutral class, D, 500 m, and for the stable classes, E-G, 200 m, averaged over the schemes. The exception is the QNSE scheme which shows 200-400 m higher PBL-heights in these calculations.

Although the different schemes seem to capture the main features in the annual course, there are considerable differences both between simulations and observations and also in between the different simulations. Compared to the observations, the WRF simulations show a general tendency to over-predict stable atmospheric conditions. To quantify these results, the error in frequency of occurrence has been calculated for the different stability classes and is presented in Table III. For the unstable classes A and B the MYNN2 scheme has the lowest frequency error and predicts class A and B to occur respectively -1.8 % less and +0.2 % more compared with FINO1 data, while the QNSE-scheme performs poorest for these two classes with a frequency error of -9.0 % and -2.7 %. For the near neutral conditions, classes C, D, and E, the MYJ scheme shows the lowest bias with -1.5 %, +0.8 %, and +1.4 %. In stable conditions, classes F and G, the QNSE and MYJ schemes outperform the rest, with a bias of respectively +2.6 % and -3.4 % for the QNSE scheme and +4.1 % and

+2.0 % for the MYJ scheme for these two classes. The ACM2 has with a bias of +8.6 % and +8.9 % clearly the poorest performance in stable atmospheric conditions.

From these results an acceptable frequency error should be below +/- 5 %. They show that e.g. the QNSE scheme, which is specifically developed for stable stratification, get high scores in such conditions. However, as also shown in part I, the prediction ability for the 100 m wind speed is not as good. ACM2, the explicit non-local closure scheme, behaves well in unstable atmospheric conditions, but both the ACM2 and QNSE schemes perform rather poor in atmospheric conditions they are not tailored for. The MYNN2 scheme is very good in predicting correctly unstable conditions, which is somewhat surprising due to its local closure nature. The YSU scheme shows medium to low performance. A correction for the stably stratified atmosphere in the YSU scheme, available in the newer version WRF3.4.1, has not been tested here. This modification might improve its performance. Again the MYJ scheme is overall the best one, with moderate performance in unstable conditions, but good performance for both near neutral and stable cases. For a local closure scheme, the better performance for neutral and stable conditions is in general expected.

Table III. Frequency error for the PGT-classes at FINO1 for the year 2005. Text in **bold** shows the best results.

	YSU	ACM2	MYJ	MYNN2	QNSE
A - Very unstable					
Frequency at FINO1: 20.5 %					
Freq. error pr. class	-6.5 %	-4.0 %	-5.0 %	**-1.8 %**	-9.0 %
Freq. error pr. class of total FINO1 data	-1.3 %	-0.8 %	-1.0 %	**-0.4 %**	-1.8 %
B - Unstable					
Frequency at FINO1: 9.5 %					
Freq. error pr. class	-1.5 %	-1.5 %	-1.8 %	**0.2 %**	-2.7 %
Freq. error pr. class of total FINO1 data	-0.1 %	-0.1 %	-0.2 %	**0.0 %**	+0.3 %
C - Weakly unstable					
Frequency at FINO1: 18.6 %					
Freq. error pr. class	-1.4 %	-8.1 %	-1.5 %	-4.8 %	**-1.0 %**
Freq. error pr. class of total FINO1 data	-0.3 %	-1.5 %	-0.3 %	-0.9 %	**-0.2** %
D - Neutral					
Frequency at FINO1: 25.1 %					
Freq. error pr. class	-4.4 %	-4.2 %	**0.8 %**	-6.7 %	8.4 %
Freq. error pr. class of total FINO1 data	-1.1 %	-1.1 %	**0.2 %**	-1.8 %	2.1 %
E - Weakly stable					
Frequency at FINO1: 4.6 %					
Freq. error pr. class	0.7 %	**0.3 %**	1.4 %	0.9 %	2.5 %
Freq. error pr. class of total FINO1 data	0.0 %	**0.0 %**	0.1 %	0.0 %	0.1 %
F - Stable					
Frequency at FINO1: 5.3 %					
Freq. error pr. class	5.1 %	8.6 %	4.1 %	3.1 %	**2.6 %**
Freq. error pr. class of total FINO1 data	0.3 %	0.5 %	0.2 %	0.2 %	**0.1 %**
G - Very stable					
Frequency at FINO1: 16.4 %					
Freq. error pr. class	8.0 %	8.9 %	**2.0 %**	9.2 %	-3.4 %
Freq. error pr. class of total FINO1 data	1.3 %	1.5 %	**0.0 %**	1.5 %	-0.6 %

4. CONCLUDING REMARKS

This study has to be seen as a continuation and deepening of the study on 100 m wind speed and wind shear presented in part I, focusing on PBL-height and atmospheric stability conditions in the MABL. A one year simulation with the mesoscale model WRF has been performed, with focus on the Marine Boundary Layer over Southern North Sea. The

Wind Energ. 2013; **00**:1–14 © 2013 John Wiley & Sons, Ltd.
DOI: 10.1002/we
Prepared using weauth.cls

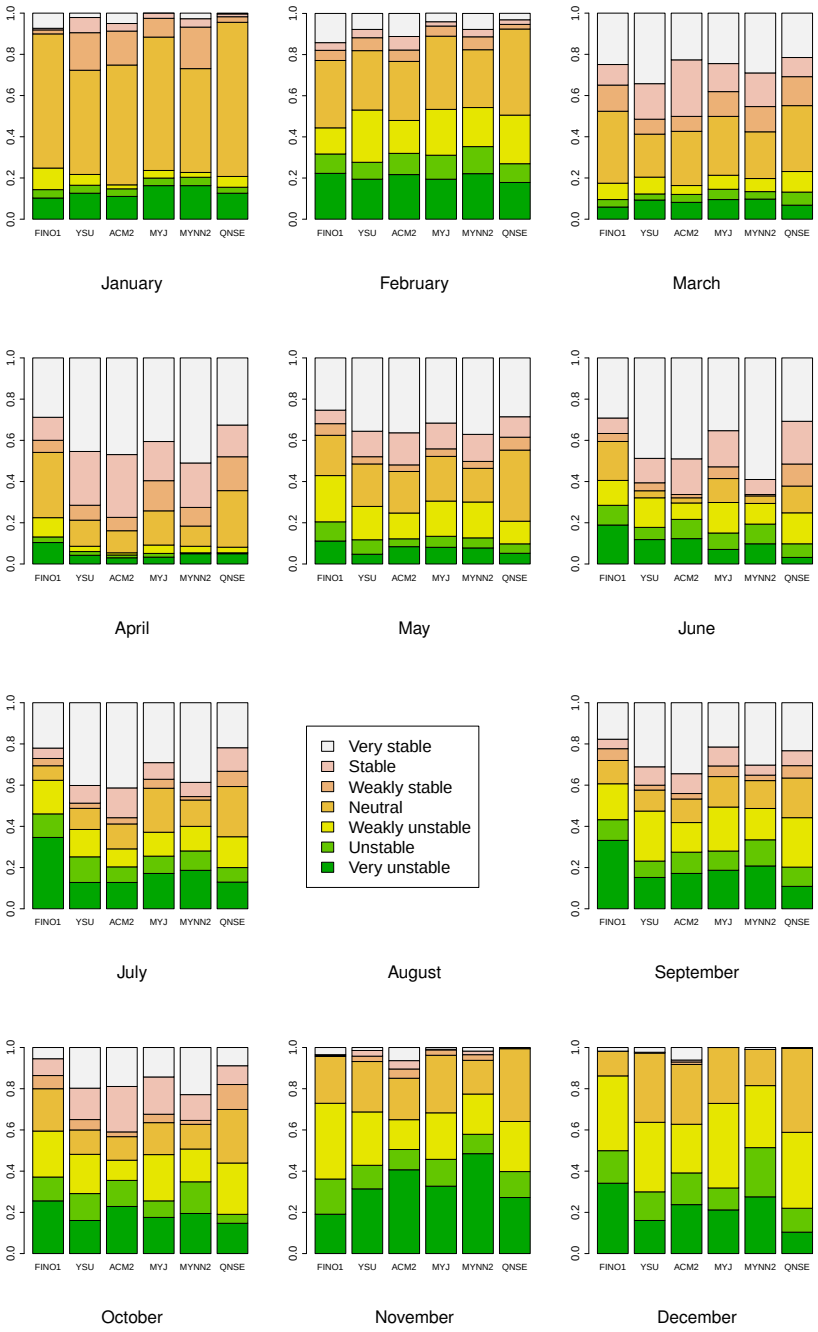

Figure 4. Frequency of occurrence of different stability classes at FINO1 for the year 2005. August has not been included in the investigation due to missing temperature data from FINO1.

output from WRF with five different planetary boundary layer schemes has been validated against observations from the meteorological research platform FINO1, situated 45 km north of the German coast.

It is not only the actual wind speed which is important when dealing with wind turbines. The atmospheric stability, and hence the turbulence, plays a crucial role for fatigue load and power output. The most critical and difficult atmospheric conditions to deal with occur when the MABL is stably stratified. The turbulence intensity is normally low in such

conditions, but the wind shear can be large over a 150-200 m turbine blade. The results show that the QNSE scheme is able to predict the frequency of stable atmospheric conditions best, with an error of only around +/- 3 % compared with FINO1 observations, but it has distinctly higher errors for near neutral and unstable conditions, up to 9 %. Looking at all stability conditions, it is again the MYJ scheme which performs best.

The modeled PBL-height calculations show a bi-modal distribution during spring and summer, with a major peak at 200-300 m, indicating stable atmospheric conditions due to warm continental air being advected over the relative cold sea. A secondary peak is found at 800-1000 m, likely associated with the frequent occurrence of a Stratocumulus-topped boundary layer. The QNSE scheme predicts in general a PBL-height several hundreds of meters higher than the other PBL-schemes. Modeled PBL-height could only be verified against the FINO1 measurements for stable situations, i.e. for PBL-heights below the mast top at 100 m. A comparison of the PBL-height of the different schemes using the implicit PBL definition of each scheme results in large differences. The results converge and come closer to the observations when a standardized method for the computation of the PBL-height is used. The study also clearly reveals the seasonal dependency of atmospheric stability over the Southern North Sea. During winter time the MABL is more or less neutral with several episodes of unstable periods. During spring and early summer the occurrence of periods with very stable stratification becomes dominant with stable conditions up to 40-45% of the time when warm continental air is coming from the South. These high values are anticipated to decrease when moving further offshore.

In 2005 the FINO1 observations showed stable MABL conditions 22% of the time (class F+G). In general this value agrees well with results from corresponding investigations in the central to northern European region, although it has to be kept in mind that the different studies might have used different stability definitions and stability determination methods. For Horns Rev, 18 km west of Jutland, Denmark, stable atmospheric conditions were determined for 7% of the time during 2004 [11]. At the same site 45% stable conditions have been reported for the time period October 2001 to April 2002. For the year 2004 the corresponding value for FINO1 has been calculated as 32% [12]. At Nysted wind farm, south of the Danish island of Lolland, stable conditions were estimated to over 35% of the time from 2004 and until May 2006,[24].

Since each PBL scheme has many different constants and parameters, a step forward in improving their performance, and at the same time improving the understanding of the MABL, is to go into more details of the schemes. One study showed promising results with a method for enhancing the TKE in the MYJ scheme, giving more correct results for the TKE in hub height in stable conditions, [25]. J W. Nielsen-Gammon et. al. reported that: *"data assimilation methods are capable of extracting significant information about parameterization behavior from the observations, and thus can be used to estimate model parameters while they adjust the model state"*, [26]. In that paper 10 parameters in the ACM2 scheme were tested, and it was found that the three most sensitive parameters in the ACM2 scheme were an exponent in the formulation of the boundary layer scaling vertical eddy diffusivity, the value of the minimum eddy diffusivity, and the critical Richardson number that defines the PBL height. In the future such types of fundamental research need to go hand in hand with tailored measurement campaigns.

In the parameter space investigated in this study, and with respect to 100 m level wind speed and wind shear investigated in Part I, the MYJ scheme can be recommended as first choice for future investigations related to offshore wind and atmospheric stability in the North Sea region without a-priori knowledge about the stability. The QNSE scheme perform very well in stable atmospheric conditions, both for wind shear and in predicting the correct stability regime when the atmosphere is in a stable mode. This is documented in both Part I and II. However, it is of concern that the QNSE scheme predicts a too high PBL-height. As the size of future offshore wind turbines is likely to increase this may be an issue when e.g. studying fatigue loads caused by the turbulence in the MABL.

ACKNOWLEDGEMENTS

This work has been partially funded by Norwegian Centre for Offshore Wind Energy (NORCOWE) under grant 193821/S60 from Research Council of Norway (RCN). NORCOWE is a consortium with partners from industry and

science, hosted by Christian Michelsen Research. Acknowledgments also go to The Research Council of Norway and StormGeo for fundings under the industrial PhD scheme. Data from FINO1 were kindly provided by Deutches Windenergie-Institute (DEWI) in Germany. Acknowledgment goes also to Uni Computing in Bergen, Norway, for access to supercomputing facilities.

REFERENCES

1. Garratt J. The internal boundary layer — A review. *Boundary-Layer Meteorology* 1990; **50**(1-4):171–203, doi:10.1007/BF00120524. URL http://dx.doi.org/10.1007/BF00120524.
2. Emeis S, Schafer K, Munkel C. Surface-based remote sensing of the mixing-layer height a review. *Meteorologische Zeitschrift* 2008; **17**(5):621–630, doi:10.1127/0941-2948. URL http://www.ingentaconnect.com/content/schweiz/mz/2008/00000017/00000005/art00009.
3. Bonin T, Chilson P, Zielke B, Fedorovich E. Observations of the Early Evening Boundary-Layer Transition Using a Small Unmanned Aerial System. *Boundary-Layer Meteorology* 2013; **146**(1):119–132, doi:10.1007/s10546-012-9760-3. URL http://dx.doi.org/10.1007/s10546-012-9760-3.
4. Coniglio MC, Correia Jr J, Marsh PT, Kong F. Verification of convection-allowing WRF model forecasts of the planetary boundary layer using sounding observations. *Weather and Forecasting* 2013; (2013). URL http://journals.ametsoc.org/doi/abs/10.1175/WAF-D-12-00103.1.
5. Floors R, Vincent C, Gryning SE, Peña A, Batchvarova E. The Wind Profile in the Coastal Boundary Layer: Wind Lidar Measurements and Numerical Modelling. *Boundary-Layer Meteorology* 2013; **147**(3):469–491, doi:10.1007/s10546-012-9791-9. URL http://dx.doi.org/10.1007/s10546-012-9791-9.
6. Peña A, Gryning SE, Hahmann A. Observations of the atmospheric boundary layer height under marine upstream flow conditions at a coastal site. *Journal of Geophysical Research: Atmospheres* 2013; **118**(4):1924–1940, doi:10.1002/jgrd.50175. URL http://dx.doi.org/10.1002/jgrd.50175.
7. Gryning SE, Batchvarova E. Marine Boundary Layer And Turbulent Fluxes Over The Baltic Sea: Measurements And Modelling. *Boundary-Layer Meteorology* 2002; **103**(1):29–47, doi:10.1023/A:1014514513936. URL http://dx.doi.org/10.1023/A:1014514513936.
8. Batchvarova E, Cai X, Gryning SE, Steyn D. Modelling Internal Boundary-Layer Development in a Region with a Complex Coastline. *Boundary-Layer Meteorology* 1999; **90**(1):1–20, doi:10.1023/A:1001751219627. URL http://dx.doi.org/10.1023/A:1001751219627.
9. Garratt J. The stably stratified internal boundary layer for steady and diurnally varying offshore flow. *Boundary-Layer Meteorology* 1987; **38**(4):369–394, doi:10.1007/BF00120853. URL http://dx.doi.org/10.1007/BF00120853.
10. Barthelmie RJ. The effects of atmospheric stability on coastal wind climates. *Meteorological Applications* 1999; **6**(1):39–47, doi:10.1017/S1350482799000961. URL http://dx.doi.org/10.1017/S1350482799000961.
11. Peña A, Gryning SE, Hasager C. Measurements and Modelling of the Wind Speed Profile in the Marine Atmospheric Boundary Layer. *Boundary-Layer Meteorology* 2008; **129**(3):479–495, doi:10.1007/s10546-008-9323-9. URL http://dx.doi.org/10.1007/s10546-008-9323-9.
12. Tambke J, Claverie L, Bye J, *et al.*. Offshore Meteorology for Multi-Mega-Watt Turbines. *Proc. European Wind Energy Conference*, 2006.
13. Neumann T, Emeis S, Illig C. Report on the Research Project OWID–Offshore Wind Design Parameter. *Wind Energy: Proceedings of the Euromech Colloquium*, Springer, 2006; 81.
14. Cheng Y, Canuto V, Howard A. An improved model for the turbulent PBL. *Journal of the Atmospheric sciences* 2002; **59**(9):1550–1565. URL http://journals.ametsoc.org/doi/abs/10.1175/

1520-0469(2002)059<1550:AIMFTT>2.0.CO;2.

15. Cheng Y, Canuto V, Howard A, Kantha LH. Comments on: On an improved model for the turbulent PBL. Author's reply. *Journal of the atmospheric sciences* 2003; **60**(24):3043–3049. URL http://journals.ametsoc.org/doi/abs/10.1175/1520-0469(2003)060<3043:COOAIM>2.0.CO;2.
16. Driedonks A, Duynkerke P. Current problems in the stratocumulus-topped atmospheric boundary layer. *Boundary-Layer Meteorology* 1989; **46**(3):275–303, doi:10.1007/BF00120843. URL http://dx.doi.org/10.1007/BF00120843.
17. Shin H, Hong SY. Intercomparison of Planetary Boundary-Layer Parametrizations in the WRF Model for a Single Day from CASES-99. *Boundary-Layer Meteorology* 2011; **139**(2):261–281, doi:10.1007/s10546-010-9583-z. URL http://dx.doi.org/10.1007/s10546-010-9583-z.
18. Fairall CW, Bradley EF, Godfrey JS, Wick GA, Edson JB, Young GS. Cool-skin and warm-layer effects on sea surface temperature. *Journal of Geophysical Research: Oceans* 1996; **101**(C1):1295–1308, doi:10.1029/95JC03190. URL http://dx.doi.org/10.1029/95JC03190.
19. Pasquill F. The estimation of the dispersion of windborne material. *Meteorol. Mag.* 1961; **90**(1063):33–49.
20. Turner DB. A diffusion model for an urban area. *Journal of Applied Meteorology* 1964; **3**(1):83–91. URL http://journals.ametsoc.org/doi/abs/10.1175/1520-0450(1964)003<0083:ADMFAU>2.0.CO;2.
21. Mohan M, Siddiqui T. Analysis of various schemes for the estimation of atmospheric stability classification. *Atmospheric Environment* 1998; **32**(21):3775–3781, doi:10.1016/S1352-2310(98)00109-5. URL http://www.sciencedirect.com/science/article/pii/S1352231098001095.
22. Carson D, Richards P. Modelling surface turbulent fluxes in stable conditions. *Boundary-Layer Meteorology* 1978; **14**(1):67–81, doi:10.1007/BF00123990. URL http://dx.doi.org/10.1007/BF00123990.
23. Golder D. Relations among stability parameters in the surface layer. *Boundary-Layer Meteorology* 1972; **3**(1):47–58, doi:10.1007/BF00769106. URL http://dx.doi.org/10.1007/BF00769106.
24. Barthelmie RJ, Jensen LE. Evaluation of wind farm efficiency and wind turbine wakes at the Nysted offshore wind farm. *Wind Energy* 2010; **13**(6):573–586, doi:10.1002/we.408. URL http://dx.doi.org/10.1002/we.408.
25. Foreman R, Emeis S. A Method for Increasing the Turbulent Kinetic Energy in the Mellor–Yamada–Janjić Boundary-Layer Parametrization. *Boundary-Layer Meteorol.* 2012; **145**(2):329–349, doi:10.1007/s10546-012-9727-4. URL http://dx.doi.org/10.1007/s10546-012-9727-4.
26. Nielsen-Gammon JW, Hu XM, Zhang F, Pleim JE. Evaluation of planetary boundary layer scheme sensitivities for the purpose of parameter estimation. *Mon. Wea. Rev.* 2010; **138**(9):3400–3417.